Therapeutic stem cells expressing variants of EGFR-specific nanobodies have antitumor effects

Jeroen A. J. M. van de Water[a,b,c], Tugba Bagci-Onder[a,b], Aayush S. Agarwal[a,b], Hiroaki Wakimoto[a,b,d], Rob C. Roovers[c], Yanni Zhu[a,b], Randa Kasmieh[a,b], Deepak Bhere[a,b], Paul M. P. Van Bergen en Henegouwen[c], and Khalid Shah[a,b,e,f,1]

[a]Molecular Neurotherapy and Imaging Laboratory, and Departments of [b]Radiology, [e]Neurology, and [d]Neurosurgery, Massachusetts General Hospital, Harvard Medical School, Boston, MA 02129; [c]Cell Biology, Department of Biology, Science Faculty, Utrecht University, 3508, Utrecht, The Netherlands; and [f]Harvard Stem Cell Institute, Harvard University, Cambridge, MA 02138

Edited by Webster K. Cavenee, Ludwig Institute for Cancer Research, University of California at San Diego, La Jolla, CA, and approved August 28, 2012 (received for review February 17, 2012)

The deregulation of the epidermal growth factor receptor (EGFR) has a significant role in the progression of tumors. Despite the development of a number of EGFR-targeting agents that can arrest tumor growth, their success in the clinic is limited in several tumor types, particularly in the highly malignant glioblastoma multiforme (GBM). In this study, we generated and characterized EGFR-specific nanobodies (ENb) and imageable and proapoptotic ENb immunoconjugates released from stem cells (SC) to ultimately develop a unique EGFR-targeted therapy for GBM. We show that ENbs released from SCs specifically localize to tumors, inhibit EGFR signaling resulting in reduced GBM growth and invasiveness in vitro and in vivo in both established and primary GBM cell lines. We also show that ENb primes GBM cells for proapoptotic tumor necrosis factor-related apoptosis-inducing ligand (TRAIL)-induced apoptosis. Furthermore, SC-delivered immunoconjugates of ENb and TRAIL target a wide spectrum of GBM cell types with varying degrees of TRAIL resistance and significantly reduce GBM growth and invasion in both established and primary invasive GBM in mice. This study demonstrates the efficacy of SC-based EGFR targeted therapy in GBMs and provides a unique approach with clinical implications.

The binding of ligands to the epidermal growth factor receptor (EGFR), a transmembrane glycoprotein, leads to activation of the EGFR tyrosine kinase and subsequent stimulation of signal transduction pathways that are involved in regulating cell proliferation, differentiation, migration, and survival (1). Although present in normal cells, EGFR is overexpressed and mutated in a variety of tumors and has been associated with poor prognosis and decreased survival (2). Over the past two decades, much effort has been directed at developing anticancer agents that can interfere with EGFR activity and arrest tumor growth and, in some cases, cause tumor regression. The most commonly used pharmacologic approaches to inhibit EGFR signaling are small-molecule receptor tyrosine kinase inhibitors (smRTKI), like Gefinitib (Iressa, ZD1839) and Erlotinib (Tarceva, OSI-774), and monoclonal antibodies (mAb), such as Cetuximab (Erbitux, Mab-C225), Panitumumab (ABX-EGF), and Matuzumab (EMD72000). Whereas smRTKI exert their effects at the intracellular domain of EGFR to prevent tyrosine kinase activity, mAbs stearically block ligand binding to the extracellular domain of the receptor (3, 4). Although the use of Erlotinib and Gefitinib have had moderate success in clinical trials in different tumor types, the use of mAbs has had limited to no success in cancer patients (3).

One aggressive tumor type with highly overactive EGFR pathway is glioblastoma multiforme (GBM), where the median survival time remains only ~1 y (5). Gene amplification of the *EGFR* and activating mutations in EGFR play a significant role in gliomagenesis and can be found in up to 70% of all GBMs (6). The mute response of anti-EGFR therapies in GBMs compared with other tumor types could be mainly attributed to the presence of the blood–brain barrier (BBB), transporter proteins, and catabolism, which are known to severely limit accumulation of the drugs at the tumor site and reduce their therapeutic efficacy (7). Therefore, there is an urgent need to develop EGFR targeting agents and to use innovative modes of delivery to enhance the efficacy of EGFR-targeting therapies for aggressive tumors like GBMs.

Recently, antibody-based anticancer therapies that involve smaller antibody fragments such as Fabs, ScFvs and nanobodies have been emerging (8). Nanobodies are derived from heavy chain-only antibodies found in camelids (e.g., *Llama glama*) and consist solely of the antigen-specific domain (V_HH) (9). These single-domain antibodies are significantly smaller in size (15 kDa) than scFv (28 kDa) or Fab (55 kDa), thereby potentially providing higher tissue dispersion than their counterparts (8). In addition, nanobodies are significantly more stable than V_H domains and have improved penetration against immune-evasive (cryptic) antigens compared with mAbs (10, 11). Nanobodies specific for EGFR have recently been developed and shown to be able to sterically hinder the binding of EGF to the receptor, thereby inhibiting EGFR signaling (12).

We and others have shown that both neural stem cells (NSC) and mesenchymal stem cells (MSC) specifically home to tumors (13, 14) and have used this tropism for on-site delivery of therapeutic proteins in mouse tumor models (15, 16). Recently, we have shown the potential of engineered stem cell based therapeutics in a clinically relevant model of tumor resection and invasiveness (17). In this study, we have engineered different bivalent EGFR targeting nanobodies (ENbs) and their imageable and proapoptotic immunoconjugates for extracellular release from stem cells (SC) and extensively characterized them in vitro. Using tumor models of malignant and primary invasive GBM, we have assessed ENb pharmacokinetics in real time and the therapeutic efficacy of ENbs and its proapoptotic immunoconjugate in vivo.

Results

Neural Stem Cells Secreting Anti-EGFR Nanobodies Inhibit EGFR Signaling in Tumor Cells. To study the effect of ENbs secreted by mammalian cells on EGFR-mediated signaling in vitro and its effect on tumor progression, we generated different versions of secretable ENbs. The lentiviral plasmid constructs consisting of an N-terminal human Flt3 signal sequence (SS) fused to bivalent and bispecific ENbs (7D12/38G7 and 7D12/9G8; from here on called ENb1 and ENb2, respectively) are diagrammed in Fig. 1*A*. These constructs were either transfected directly into different cell types or packaged into lentivirus (LV) virions and used to create human and mouse NSC secreting ENbs. For assessing their EGFR specificity, ENbs were purified from the conditioned

Author contributions: K.S. designed research; J.A.J.M.v.d.W., T.B.-O., A.S.A., H.W., Y.Z., R.K., D.B., and K.S. performed research; R.C.R. and P.M.P.V.B.e.H. contributed new reagents/analytic tools; J.A.J.M.v.d.W., T.B.-O., A.S.A., H.W., Y.Z., R.K., D.B., and K.S. analyzed data; and J.A.J.M.v.d.W., T.B.-O., and K.S. wrote the paper.

The authors declare no conflict of interest.

This article is a PNAS Direct Submission.

[1]To whom correspondence should be addressed. E-mail: kshah@mgh.harvard.edu.

This article contains supporting information online at www.pnas.org/lookup/suppl/doi:10.1073/pnas.1202832109/-/DCSupplemental.

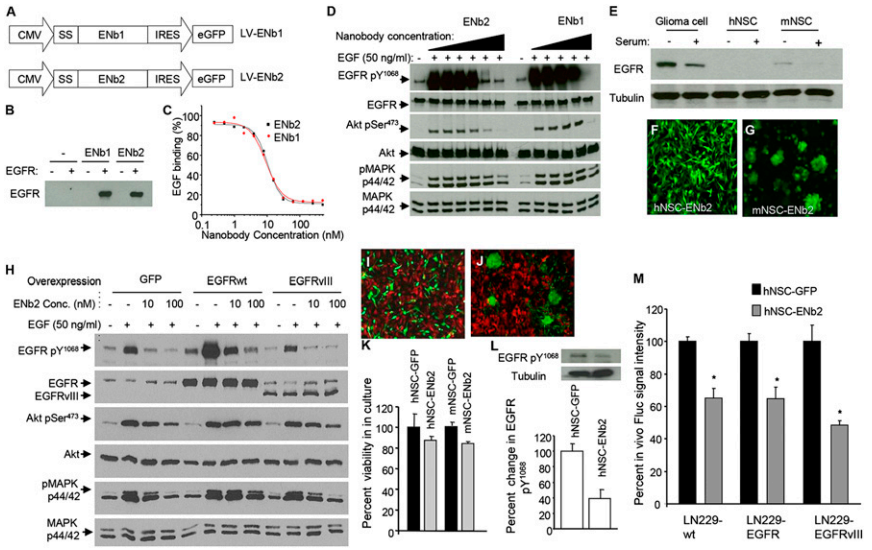

Fig. 1. Functionality of anti-EGFR nanobodies released from neural stem cells. (*A*) Schematic representation of lentiviral transfer vectors bearing anti-EGFR nanobody cDNAs. (*B*) Western blot analysis showing the EGFR specificity of nanobodies on EGFR-negative [NIH 3T3 (-)] and EGFR-positive [Her14 (+)] cell lines incubated with or without ENbs. (*C*) ELISA showing the EGF competition by anti-EGFR nanobodies. (*D*) Western blot analysis showing inhibition of EGFR activation and downstream signaling in serum-starved Her14 cells incubated anti-EGFR nanobodies. (*E*) Western blot analysis showing EGFR expression levels in NSC and U87 GBM cells. (*F* and *G*) Photomicrographs showing efficient transduction of hNSC (*F*) and mNSC (*G*) with LV-ENb2 by GFP expression on day 21 after transduction. (*H*) Western blot analysis showing inhibition of EGFR activation and downstream signaling in serum-starved LN229 GBM cells overexpressing either EGFR wt., EGFRvIII, or GFP incubated with anti-EGFR nanobodies. (*I* and *J*) Photomicrographs showing cocultured hNSC (*I*) and mNSC (*J*) expressing ENb2 (green) and LN229 GBM cells (red). (*K*) Plot showing changes in GBM cell numbers measured by changes in Fluc bioluminescence intensity when cocultured for 3 d with hNSC or mNSC expressing ENb2 or mNSC-ENb2 or GFP control. (*L*) Western blot analysis and quantification of the band intensity showing the inhibition of EGFR activation in LN229 cocultures with hNSC-ENb2 or hNSC-GFP after 72 h. (*M*) Plot showing changes in GBM growth in mice implanted with a mix of LN229-mCherry-Fluc, LN229-mCherry-Fluc overexpressing either EGFR wt., or EGFRvIII, and hNSC-ENb2 and controls NSC-GFP 72 h after implantation. Data were represented as mean ± SEM, and * denotes $P < 0.05$, Student's *t* test.

medium of LV-ENb1 or LV-ENb2 transfected HEK293T/17 cells (Fig. S1) and tested on EGFR-positive (Her14) and EGFR-negative (NIH 3T3 2.2) cell lines. Detection of EGFR immunoprecipitated by ENbs using Western blotting showed that both ENbs bound to EGFR (Fig. 1*B*). This binding of ENbs to the EGFR ectodomain prevented the binding of the ligand EGF to EGFR (Fig. 1*C*), which resulted in reduced activation of EGFR and, thereby, inhibition of signaling via the Ras/MAPK and PI3K/AKT pathways in Her14 cells (Fig. 1*D*). These results show that ENbs secreted by mammalian cells are fully functional and have the potential to be used for EGFR-targeted therapy in cancer.

Next, we explored the possibility of using neural stem cells (NSC) as delivery vehicles of ENbs. We first confirmed that both human (h) and mouse (m) NSCs expressed significantly lower levels of EGFR than the commonly used established GBM line, U87 (Fig. 1*E*). Both mNSC and hNSC were efficiently transduced with LV-ENbs as revealed by GFP fluorescence (Fig. 1 *F* and *G*), and they constantly secreted significant amounts of ENbs in the culture medium over a period of at least 3 wk as revealed by Western blotting (Fig. S2*A*). NSC-ENb were shown to retain the stem cell properties as shown by the expression of NSC marker nestin and their ability to differentiate into terminal cell types as shown by the expression of neuron specific marker, MAP-2 (Fig. S2 *B*–*E*). To explore the effect of ENbs on EGFR signaling in GBM cells, we incubated serum-starved GBM cell line LN229 (wt or engineered to overexpress EGFR or mutant EGFR variant, EGFRvIII) with various concentrations of purified ENbs and analyzed them for EGFR phosphorylation and changes in downstream signaling molecules (Fig. 1*H*). EGFR activation and signaling via the PI3K/AKT and MAPK pathways was inhibited in LN229 cells irrespective of their EGFR expression status. To determine the efficacy of NSC-delivered ENb treatment for GBMs, LN229 GBM cells, engineered to express mCherry-FLuc, were cocultured with either human (Fig. 1*I*) or mouse (Fig. 1*J*) NSC expressing GFP or ENb2. A slight reduction in LN229 proliferation was seen when cocultured with hNSC-ENb2 and mNSC-ENb2 compared with controls (Fig. 1*K*). Western blot analysis revealed that EGFR activation was significantly reduced when LN229 GBM cells were cocultured with hNSC-ENb2 compared with hNSC-GFP (Fig. 1*L*). When a mixture of LN229-mCherry-Fluc cells and hNSC-GFP or hNSC-ENb2 cells was implanted in mice, a significant reduction in the Fluc signal intensity, depicting the number of viable LN229 GBM cells, was seen in NSC-ENb2/LN229-mCherry-Fluc implanted mice compared with the controls (Fig. 1*M*). Comparable results were obtained when LN229-mCherry-Fluc cells further engineered to overexpress either EGFR or EGFRvIII (Fig. S3) were tested (Fig. 1*M*). These results show that NSC-expressed ENbs significantly inhibit EGFR and its downstream signaling pathways in GBMs and that NSC-delivered ENbs reduce GBM growth in vivo in GBM cells expressing wt-EGFR, overexpressing wt-EGFR or mutant EGFRvIII.

Pharmacokinetics of NSC-ENbs in Vitro. The concentration of EGFR targeting antibody to which tumor cells are exposed is critical for the success of anti-EGFR therapy. To study the secretion and intracellular localization of NSC-produced ENbs, we genetically fused the ENbs to *Gaussia* luciferase (GLuc) (ENb-G) or to a fusion between GLuc and the fluorescent protein mCherry (GmC) (Fig. 2*A*) and created NSC lines expressing either ENb-G or ENb-GmC. The fusion proteins ENb1-G and ENb2-G were found to be EGFR-specific and competed with EGF binding to EGFR, thus resulting in the inhibition of receptor activation (Fig. 2 *B*–*D*). NSC expressing FLuc were transduced with LV-ENb1-G and LV-ENb2-G to simultaneously analyze the efficiency of ENb secretion (GLuc signal) and NSC numbers (FLuc signal). Analysis of GLuc expression in NSC and the culture medium showed that ~65% of the ENbs were secreted in the medium (Fig. 2*E*). However, when ENb production and NSC number were correlated, ENb2-G was shown to be released from NSC twice as efficiently as ENb1-G (Fig. 2*F* and Fig. S4). To study localization of ENbs within the NSC compartments, we used ENb2-GmC–expressing NSC. ENb2 protein (mCherry expression) localized intracellularly to distinct cellular compartments (most likely before secretion) in contrast to the nucleocytoplasmic GFP expression (Fig. 2 *G*–*J*). These results show that ENbs retain functionality after fusion of imaging markers and the combined fluorescence and bioluminescence imaging provides an insight into ENb pharmacokinetics in vitro. Because of its superior secretion, we chose ENb2 to further use and characterize in the following studies.

Pharmacokinetics of ENb2-G and NSC in Vivo. To study the pharmacokinetics of NSC-delivered ENb2 in vivo, mice bearing s.c. mCherry-Fluc GBM tumors in a dorsal skinfold window chamber

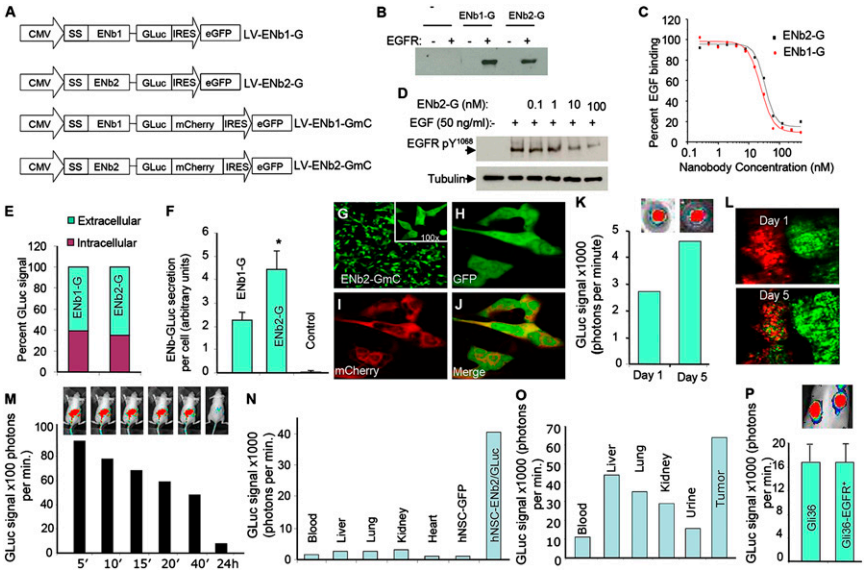

Fig. 2. Pharmacokinetics of anti-EGFR nanobodies in vitro and in vivo. (*A*) Schematic representation of lentiviral transfer vectors bearing imageable anti-EGFR nanobodies (ENb1 and ENb2) genetically fused to *Gaussia* luciferase (GLuc) or to a fusion of GLuc and mCherry. (*B*) Western blot analysis showing the EGFR specificity of GLuc nanobody variants on EGFR-negative [NIH 3T3 (-)] and EGFR-positive [Her14 (+)] cell lines incubated with or without Enb-GLuc. (*C*) ELISA showing the EGF competition by anti-EGFR Enb-GLuc variants. (*D*) Western blot analysis showing inhibition of EGFR activation by nanobody-GLuc variants on serum-starved Her14 cells incubated with serial dilutions of ENb2-G. (*E*) Gluc bioluminescence assay showing the presence of nanobody-GLuc fusion proteins intracellularly and in the culture medium in human NSC expressing ENb1-G and ENb2-G. (*F*) Dual bioluminescence assay on human NSC coexpressing GFP-FLuc and ENb1-G or ENb2-G showing the ratio of nanobody-GLuc fusion in the culture medium and the relative cell number by measurement of GLuc and FLuc activity, respectively. (*G–J*) Fluorescence confocal microscopy on hNSC expressing ENb2-GmC showing the intracellular localization of nanobodies (red) and GFP (green). (*K* and *L*) Combined intravital microscopy and bioluminescence imaging of U87-FLuc-TdTomato GBM (red)-bearing SCID mice implanted s.c. with human NSC expressing ENb2-G (green) in a dorsal skinfold window chamber. Mice were imaged on day 1 and 5 after NSC implantation by bioluminescence imaging for the secretion of ENb2-G (*K*) and by intravital microscopy for the fate of NSC (*L*). (*M*) In vivo bioluminescence imaging of purified ENb2-G injected into mice bearing established Gli36-Fluc-mCherry tumors by i.v. injection and analyzed at different time points after coelenterazine injection. (*N*) Ex vivo analysis of biodistribution of NSC-delivered ENb2-G assessed by GLuc imaging of organs. (*O*) Ex vivo analysis of biodistribution of systemically administered purified ENb2-G assessed by GLuc imaging of organs. (*P*) Mice bearing Gli36-Fluc-mCherry (left flank) and the EGFR overexpressing Gli36-FLuc-mCherry-EGFR$^+$ (right flank) s.c. tumors were given purified ENb2-G protein i.v. and were imaged for GLuc. Representative image and summary graph showing localization of ENb2-G in mice. In all graphs, error bars represent SEM. Data were represented as mean ± SEM, and * denotes $P < 0.05$, Student's *t* test.

were implanted with NSC-ENb2-G at a ~1 mm distance from the tumor. Bioluminescence imaging showed the sustained on-site delivery of ENb2-G from NSC for a period of at least 5 d (Fig. 2*K*), whereas intravital microscopy on that same set of mice showed the close proximity of NSC-ENb2-G to the tumor cells (Fig. 2*L*). Serial bioluminescence imaging of systemically delivered ENb2-G in tumor-bearing mice revealed that after systemic delivery, the availability of ENb2-G to tumor cells decreased considerably with time and was barely present at 24 h after injection (Fig. 2*M*). To compare the in vivo distribution of systemically delivered ENbs and NSC-delivered ENbs, mice bearing established s.c. mCherry-FLuc tumors were either implanted with NSC expressing ENb2-G or GFP (control) or injected systemically with ENb2-G. In vivo GLuc bioluminescence imaging and correlative ex vivo analysis of various internal organs revealed that ENb2-G was mostly present in the tumor when treated with NSC-ENb2-G or systemically injected ENb2-G. However, a substantial amount of ENb2-G was also found in liver, lung, and kidney when tumor-bearing mice were systemically injected with ENb-2-G compared with NSC-ENb2-G treatment (Fig. 2 *N* and *O*). Next, to assess whether tumor localization of ENb2-G depends on EGFR expression levels, mice bearing tumors generated from wild-type Gli36 or Gli36 GBM cells modified to overexpress EGFR (17) were administered with purified ENb2-G. GLuc bioluminescence imaging showed that ENb2-G accumulated in tumors, and that the levels of EGFR expression did not affect the extent of ENb2-G localization to tumors (Fig. 2*P*). These results indicate that NSC-delivered ENb2 specifically targets tumor cells and is sustainably delivered to tumors in contrast to systemically administered ENbs.

Cytotoxic Variant of Anti-EGFR Nanobodies, ENb2-TRAIL, Efficiently Eliminates GBM Cells in Vitro. To target tumor cell proliferation and death pathways simultaneously, we engineered LVs consisting of cDNA fusions encoding ENb2 and cytotoxic secretable TRAIL recombinant protein (ENb2-TRAIL) (Fig. 3*A*). HEK-293T transduced with LV-ENb2-TRAIL efficiently secreted ENb2-TRAIL (200 ng/mL per 10^6 cells) and, when tested on Her14 (EGFR+) and NIH 3T3 (EGFR-) cell lines, ENb2-TRAIL was shown to specifically bind to EGFR (Fig. 3*B*) and compete with EGF ligand binding to EGFR (Fig. 3*C*). This EGFR-ligand binding competition resulted in the subsequent inhibition of EGFR signaling in Her14 and different GBM lines that have varying levels of resistance/sensitivity to TRAIL-induced apoptosis including LN229 cells that are most resistant to TRAIL (Fig. 3*D* and Fig. S5*A*). To explore the effect of NSC-released ENb2-TRAIL on tumor cell proliferation and death, we engineered mouse NSC (from here on called NSC) to express ENb2-TRAIL and cocultured GBM cells expressing mCherry-Fluc with NSC-ENb2-TRAIL, NSC-ENb2, and control NSC-GFP. NSC-ENb2 treatment resulted in reduced viability of all GBM cells Gli36, U87, and LN229 (Fig. 3 *E* and *F*). Furthermore, NSC-ENb2-TRAIL treatment had a profound effect on GBM cell viability and resulted in TRAIL-mediated apoptosis as indicated by caspase-3/7 up-regulation and PARP cleavage in TRAIL-sensitive (Gli36) and medial TRAIL-sensitive GBM (U87) lines (Fig. 3 *E–G* and Fig. S5*B*). Enb2-TRAIL treatment of U87 cells in which death receptor (DR) 5 was knocked down resulted in significantly reduced PARP cleavage and increased cell viability compared with controls, which indicate the interaction of ENb-TRAIL with DRs and its downstream apoptosis pathway (Fig. S6).

Next, we compared the effect of NSC-TRAIL and NSC-ENb2-TRAIL on the TRAIL-resistant GBM line, LN229. Engineered NSC cocultured in different ratios with LN229 cells showed that NSC-ENb2-TRAIL resulted in considerable reduction in GBM cell viability (Fig. 3*H*), increased caspase activation, and PARP cleavage (Fig. 3*I*) compared with NSC-TRAIL or NSC-ENb2. Together, these results indicate that the on-site delivery of ENb2 or ENb2-TRAIL via NSC (cocultures) is more effective than the NSC-conditioned medium treatment. Furthermore, NSC-released ENb2-TRAIL targets both cell proliferation and cell death pathways and has the ability to sensitize TRAIL-resistant GBM cells.

NSC-Delivered ENb2 and ENb2-TRAIL Significantly Influence GBMs in Vivo. We first tested Cetuximab, a known monoclonal antibody targeting EGFR, in our GBM models. Mice bearing U87-mCherry-Fluc GBMs were administered Cetuximab or saline for a period of 11 d and imaged for tumor volumes. There was no significant

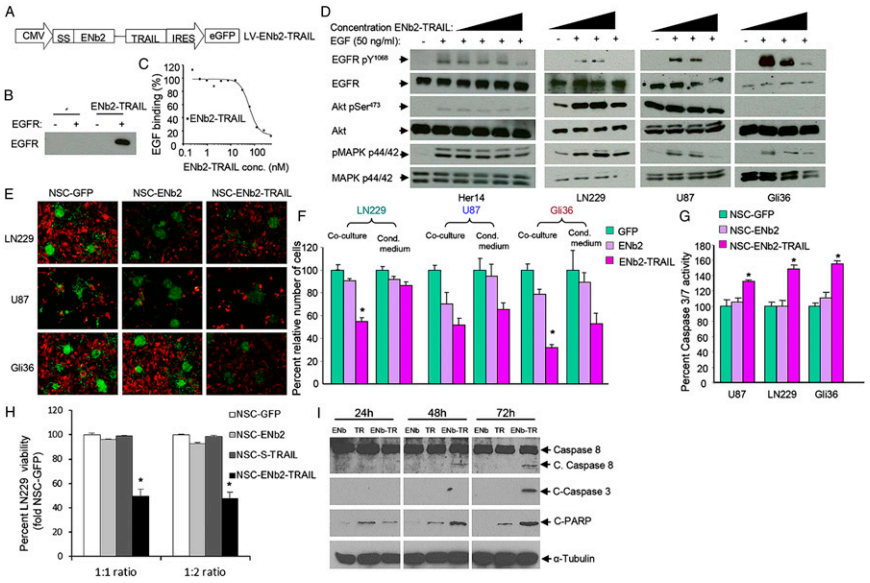

Fig. 3. Efficacy of the dual effector molecule ENb2/TRAIL. (*A*) Schematic representation of lentiviral transfer vectors bearing cytotoxic variant of EGFR nanobody, ENb2-TRAIL. (*B*) Western blot analysis showing the EGFR specificity of ENb2-TRAIL on NIH 3T3 and Her14 cell lines incubated with or without ENb2-TRAIL. (*C*) ELISA showing the EGF competition by ENb2-TRAIL. (*D*) Western blot analysis showing inhibition of EGFR and downstream signaling via the AKT and MAPK pathways on serum-starved Her14 and GBM (LN229, U87, Gli36) cells incubated with ENb2-TRAIL. (*E*) Fluorescence microscopy on FLuc-mCherry expressing GBM cells (LN229, U87, and Gli36) cocultured with mouse NSC expressing GFP (control), ENb2, or ENb2-TRAIL. (*F*) Relative GBM cell viability in coculture or after incubation with conditioned medium from mNSC expressing GFP, ENb2, or ENb2-TRAIL for 72 h as determined by measuring FLuc activity. (*G*) Caspase 3/7 activity in coculture of GBM cells and mNSC. (*H*) Relative LN229-mCherry-Fluc cell viability in coculture with mNSC expressing GFP, ENb2, S-TRAIL, or ENb2-TRAIL for 72 h as determined by measuring FLuc activity. (*I*) Western blot analysis of LN229 cells treated with mNSC expressing ENb2, S-TRAIL, or Enb-TRAIL. Data were represented as mean ± SEM and * denotes $P < 0.05$, Student's *t* test.

change in GBM growth in Cetuximab-treated mice compared with vehicle treatment (Fig. 4*A*). These results are in line with the findings from a number of preclinical and clinical studies where mice bearing GBMs and patients with GBMs were treated with Cetuximab as a single therapy (18–20). To investigate the efficacy of NSC-delivered ENbs and its cytotoxic variant ENb2-TRAIL in vivo, we first implanted a mix of U87-mCherry-FLuc GBM cells and NSC expressing only GFP and ENb2 or ENb2-TRAIL intracranially and imaged tumor burden over time. Bioluminescence imaging revealed a significant inhibition of tumor growth when treated with NSC-ENb2 compared with the controls, whereas NSC-ENb2-TRAIL–treated tumors regressed completely (Fig. S7). Because using a mixture of tumor and therapeutic stem cells is not clinically representative, we tested the therapeutic efficacy of NSC-ENb2 and NSC-ENb2-TRAIL in an established intracranial U87-mCherry-FLuc GBM model. NSC-ENb2 significantly inhibited tumor growth, and NSC-ENb2-TRAIL efficiently prevented any outgrowth of the tumor for the duration of the treatment period (Fig. 4*B*). When the therapeutic efficacy of NSC-ENb2-TRAIL was compared with NSC-S-TRAIL in established U87-mCherry-Fluc tumors, NSC-ENb2-TRAIL treatment resulted in a significant reduction in tumor volumes compared with NSC-S-TRAIL treatment (Fig. S8). The presence of therapeutic NSC was confirmed by GFP fluorescence imaging on day 4 brain sections from mCherry-expressing GBMs subjected to the different treatments (Fig. 4 *C–E*). H&E staining on brain sections also revealed a significant decrease in tumor volumes in NSC-ENb2-TRAIL and NSC-ENb2–treated mice compared with controls (Fig. 4 *F–H*). Furthermore, a significantly increased cleaved caspase-3 staining was observed in day 4 brain sections obtained from NSC-ENb2-TRAIL–treated tumors compared with NSC-ENb2 or control NSC-GFP–treated tumors, showing the involvement of caspase-mediated apoptosis (Fig. 4 *I–O*). Mice treated with control NSC-GFP showed a median survival of 44.5 d. In contrast, mice treated with control NSC-ENb2 showed a median survival of 51 d and 80% of mice treated with NSC-ENb2-TRAIL were alive

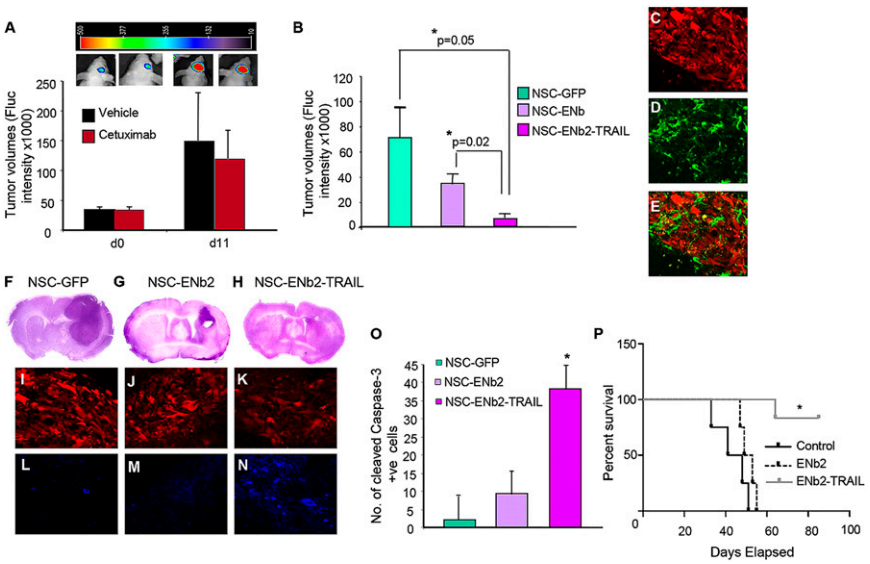

Fig. 4. In vivo efficacy of ENb2 and ENb2-TRAIL secreting NSC on GBM volumes. (*A*) Tumor volumes measured by FLuc bioluminescence imaging signal intensity of nude mice bearing U87-mCherry-FLuc intracranial tumors and injected with Cetuximab (1 mg per mouse·d^{-1}) or vehicle daily for 1 wk. (*B*) Tumor volumes of nude mice bearing established intracranial U87-mCherry-FLuc tumors treated with NSC expressing GFP, ENb2, or ENb2-TRAIL. (*C–E*) Photomicrographs show presence of NSC (green) within U87-mCherry-Fluc tumors (Red). (*F–K*) Photomicrographs of H&E stained and fluorescence microscopy analyzed sections of the brain of GBM-bearing mice treated with NSC-GFP (*F* and *I*), NSC-ENb2 (*G* and *J*), and NSC-ENb2-TRAIL (*H* and *K*) showing the changes in tumor volumes and mCherry+ tumor cells. (*L–O*) Photomicrographs (*L–N*) and plot (*O*) showing the extent of cleaved caspase-3 staining (blue) in brain sections of NSC-GFP (*L*), NSC-ENb2 (*M*), and NSC-ENb2-TRAIL (*N*) treated mice. Plot shows the number of cleaved caspase-3 cells in different treatment groups (*O*). (Original magnification: 20x.) (*P*) Kaplan–Meier survival curves of mice bearing established tumors and implanted with NSC expressing GFP, ENb2, or ENb2-TRAIL intratumorally ($n = 5$ per group). For *A* and *B*, data were represented as mean ± SEM, and * denotes $P < 0.05$, Student's *t* test. For *P*, * denotes $P < 0.05$ as compared Enb2 and control groups, log-rank test.

80 d after treatment (Fig. 4*P*). These results reveal that tumor-itropic NSC-releasing ENb2 inhibits GBM growth and that the efficacy of ENb2-based therapy is enhanced by NSC releasing ENb2-TRAIL.

ENb2 and ENb2-TRAIL Inhibit Invasiveness of Primary GBM Tumor Cells. Because increased invasion is one of the major impediments to successful therapies in malignant GBM, we sought to evaluate whether our therapeutic NSC can suppress GBM cell invasiveness in vivo. To this end, we used a xenograft mouse model, generated with CD133-positive primary GBM cells, that recapitulates the clinical settings of tumor cell invasiveness (21). Mice bearing intracranial GBM8-mCherry-FLuc tumors were implanted with NSC expressing either only GFP or ENb2 or ENb2-TRAIL intratumorally. Mice were killed at different days after NSC implantation, and brain sections were visualized for NSC (GFP+) and tumor cells (mCherry+). A mixed presence of tumor cells and NSC was seen at the implantation site on day 1 after NSC implantation (Fig. 5 *A* and *B*). Brain sections from mice killed on day 7 after NSC implantation revealed that NSC-GFP tracked invading GBM8 cells (Fig. 5 *C–E*). Furthermore, NSC-ENb2 significantly inhibited tumor invasiveness by 60%, and NSC-ENb2-TRAIL further suppressed the tumor cell invasion because almost no mCherry+ cells migrated out to the paraventricular area (Fig. 5*F*). In contrast, from the tumors treated with control NSC, a significant number of GBM cells migrated/invaded along the white matter tract and reached an area adjacent to the lateral ventricle, indicating that the highly invasive property of the primary GBM cells was not affected by control NSC (Fig. 5 *B–F*). We also tested the broader therapeutic efficacy of ENb2-TRAIL on our patient-derived GBM lines. A significant decrease in GBM cell viability was seen in most of the GBM lines treated with ENb2-TRAIL compared with ENb2 and control treatment (Fig. S9). These results reveal that NSC track invasive GBM cells in the brain and that ENb2 released by NSC inhibits invasiveness of primary GBM cells, which is further enhanced by the ENb2-TRAIL variant.

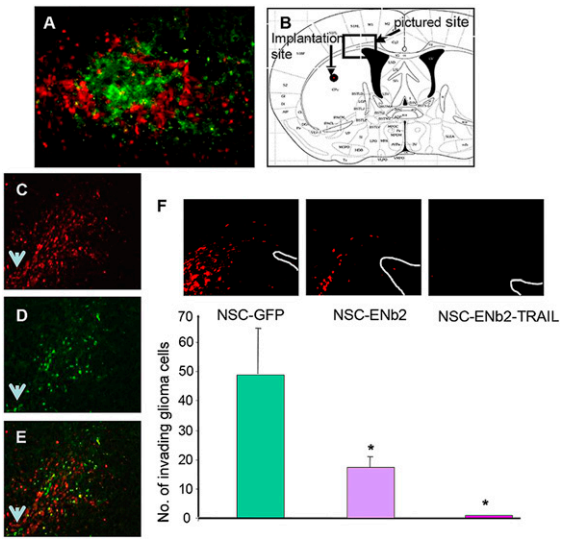

Fig. 5. In vivo efficacy of ENb2 and ENb2-TRAIL on inhibiting invasiveness of primary GBM cells. (*A*) Photomicrograph showing the presence of both NSC (green) and GBM cells (red) in brain sections from GBM8-mCherry-Fluc bearing nude mice intracranially implanted with mNSC-GFP at the cell implantation site day 1 after mNSC implantation. (*B*) A schematic of the mouse brain showing the implantation site (shown in *A*) and the site adjacent to the lateral ventricle where GBM cell migration was evaluated (pictured in *C–E*). (*C–E*) Photomicrographs showing the invasiveness of GBM8-mCherry cells (*C*) and the tracking of GBM8-mCherry-cells by NSC-GFP (*D* and *E*) on day 7 after NSC-GFP implantation. (*F*) Representative photomicrographs and plot showing the number of GBM8-mCherry invading cells to the site (shown in *B*) 7 d after NSC-GFP, NSC-ENb2, and NSC-ENb2-TRAIL treatment. Arrows indicate the site of GBM8 and NSC implantation (*C–E*), and white lines indicate the wall of the lateral ventricle (*F*). For *F*, data were represented as mean ± SEM, * denotes $P < 0.05$, Student's *t* test.

Discussion

In this study, we assessed the therapeutic efficacy of EGFR-targeting nanobodies and their imageable and proapoptotic variants in vitro and in mouse models of malignant and invasive GBMs. We show that SC-delivered ENbs localize to tumors and that sustained release of ENbs from SCs inhibits EGFR signaling, reduces GBM growth, and primes TRAIL-resistant GBM cells to TRAIL-mediated apoptosis. Furthermore, SC delivered immunoconjugate of ENb and TRAIL targets a wide spectrum of GBM cells with varying degrees of TRAIL resistance by targeting both cell death and survival pathways in established malignant and primary invasive mouse GBM models.

Despite efforts to improve the drug delivery across the BBB, the efficacy of anti-EGFR therapies for GBMs has been limited (19). These highly specific antibody fragments are relatively small with a size of only 15 kDa and, therefore, have higher tissue dispersion than mAbs (20) and do not elicit an immune response in the host. Also, some nanobodies are known to cross the BBB fairly easily (21, 22) and are therefore potentially better therapeutic agents than mAb or smRTKI for the treatment of brain malignancies. We and others (13, 14) have shown that NSC and MSC migrate extensively toward brain tumors and, therefore, have an enormous therapeutic potential as gene delivery vehicles (15, 23). In this study, we armed NSC with ENb and ENb-derived immunoconjugates and showed that transgene expression is maintained in vitro and in vivo over a period without affecting stem cell properties. NSC released ENbs-inhibited EGFR signaling in vitro and also resulted in a strong reduction of tumor growth in GBM-bearing mice. Interestingly, a more significant effect of ENb2 on GBM cell growth was observed in vivo than in culture conditions, which could possibly be due to the amplification of EGFR and gain of EGFR-dependence of tumor cells in mouse tumor models (24).

Although the in vitro response of GBM cell lines to anti-EGFR nanobodies is not directly predictive of the in vivo response, our data gives us insights about the downstream components of EGFR signaling. For example, U87 cells have a frame-shift mutation in the gene encoding PTEN, a tumor suppressor and a negative modulator of cell growth through inhibition of AKT signaling, rendering it inactive and reducing ligand-induced EGFR degradation (25). In accordance, although ENbs did not strongly affect the AKT activation in these cells, their inhibitory effects on the EGFR activation and MAPK p44/42 pathway were significant. In contrast, LN229 cells, which have wild-type PTEN, showed inhibition of both AKT and MAPK p44/42 pathways with ENb treatment. PTEN status of tumors has been reported to affect the tumor response to EGF receptor tyrosine kinase inhibitor-based therapies in patients (26, 27). Our results indicate that the PTEN status of tumor cell lines alone does not predict the sensitivity of a tumor to ENb-based therapies. Therefore, it is tempting to speculate that NSC delivering anti-EGFR nanobodies provide maximal EGFR inhibition that may overcome resistance to EGFR-targeting therapies conferred by mutations in PTEN or PI3-kinase (25).

Our in vivo studies with NSC-ENbs reveal that on-site delivery of ENbs within the tumors inhibit tumor growth but does not result in a significant regression of the tumor. These data is consistent with previous studies on EGFR-inhibiting drugs, which have been shown to work mostly in combination with therapies like radiation and chemotherapy (28). To increase the efficacy of anti-EGFR nanobody-mediated therapy by simultaneously targeting the cell proliferation and death pathways, we designed the immunoconjugate ENb2-TRAIL. Our results reveal that ENb2-TRAIL induces caspase-3/7-mediated apoptosis in GBM cell lines with various degrees of TRAIL resistance. Interestingly, survival of the TRAIL-resistant cell line LN229 was significantly affected by ENb2-TRAIL, indicating that

simultaneous EGFR inhibition might sensitize this cell line to TRAIL-induced apoptosis. Another interesting observation made in this study is that the efficacy of the treatment largely depends on how the drugs are delivered to tumor cells. Our results indicate that continuous exposure of tumor cells to ENbs is more effective than a single high-dose treatment. These observations further strengthen the rationale of using NSCs as delivery vehicles for sustained expression and release of therapeutics. Besides, ENb2-TRAIL was shown to be a highly effective therapeutic molecule in our mouse models, leading to tumor regression or stable disease.

For accurate diagnosis of tumors and tumor locations, strong imaging tools with high specificity are essential. Antibodies directed against tumor-specific epitopes have been shown to have great potential for tumor imaging (29). Recently, the potential of monovalent anti-EGFR nanobodies for tumor imaging using SPECT was examined and it was shown that the nanobodies home to EGFR-overexpressing tumors (6, 30). In the current study, we explored the potential of using bivalent and bispecific anti-EGFR nanobodies for tumor localization by using bioluminescence imaging modalities and show that the nanobodies localize to EGFR-expressing tumors. Systemic administration of drugs does not ensure tumor-specific targeting, and often these compounds accumulate at high levels in kidneys and liver, causing renal and liver failure (31, 32). Using the imageable variant of ENbs and noninvasive bioluminescence imaging, we show that, in contrast to i.v. administered ENbs, NSC-delivered ENbs specifically localize to the tumor environment and do not distribute systemically and are released in situ sustainably.

In conclusion, our studies reveal the potential of on-site delivered anti-EGFR therapies for brain tumors. NSC-delivered anti-EGFR nanobodies inhibit tumor cell proliferation and migration and, combined with cytotoxic molecules, significantly enhance therapeutic outcome. In addition, anti-EGFR nanobodies are good candidates for diagnostics and tumor localization.

Materials and Methods

Therapeutic Efficacy Studies in Vivo. ***Cetuximab studies.*** U87-mCherry-FLuc cells were stereotactically implanted into the brains of nude mice (2×10^5 cells per mouse; $n = 6$). Daily i.p. administration of Cetuximab (40 mg/kg; ImClone Systems) or saline vehicle was performed ($n = 3$ per group) for 11 d, and tumor volumes were determined by Fluc bioluminescence imaging as described (33).

Efficacy of therapeutic NSC mixed with GBM cells. U87-mCherry-FLuc were mixed with NSC-GFP, NSC-ENb2, or NSC-ENb2-TRAIL and either implanted s.c. or stereotactically into the right frontal lobe of nude mice (from bregma: –2 mm lateral, –2 mm ventral). Mice ($n = 3$ per group) were imaged for FLuc activity as described (44).

Efficacy of therapeutic NSC on established intracranial tumor. U87-mCherry-FLuc cells (1×10^5) were stereotactically implanted into the right frontal lobe of nude mice (from bregma: –2 mm lateral, –2 mm ventral). Mice bearing established tumors (as determined by Fluc bioluminescence imaging) were implanted with NSC expressing GFP, ENb2, or ENb2-TRAIL (5×10^5) intratumorally ($n = 7$ per group), followed by a second implantation on day 7. Mice were imaged for FLuc activity as described (16). For survival studies, mice bearing established tumors were implanted with NSC expressing GFP, ENb2, or ENb2-TRAIL (5×10^5) intratumorally ($n = 5$ per group) and followed for survival. All animal studies have been approved by the Institutional Animal Care and Use Committee at Massachusetts General Hospital.

Statistical Analysis. Data were analyzed by Student's *t* test when comparing two groups. Data were expressed as mean ± SEM, and differences were considered significant at $P < 0.05$. Survival times of groups of mice were compared by using a log-rank test.

Additional methods are described in detail in *SI Materials and Methods*.

ACKNOWLEDGMENTS. We thank Dr. Cedric Berger for his help with FACS analysis. This work was supported by National Institutes of Health (NIH) Grant R21 CA86355 (to K.S.), NIH Grants R01 CA138922 and R01 NS071197 (to K.S.), the American Cancer Society (K.S.), the Dutch Cancer Society (J.A.J. M.v.d.W.), and The James McDonald Foundation (K.S.).

1. Citri A, Yarden Y (2006) EGF-ERBB signalling: Towards the systems level. *Nat Rev Mol Cell Biol* 7:505–516.
2. Ciardiello F, Tortora G (2008) EGFR antagonists in cancer treatment. *N Engl J Med* 358: 1160–1174.
3. Martinelli E, De Palma R, Orditura M, De Vita F, Ciardiello F (2009) Anti-epidermal growth factor receptor monoclonal antibodies in cancer therapy. *Clin Exp Immunol* 158:1–9.
4. Sato JD, et al. (1983) Biological effects in vitro of monoclonal antibodies to human epidermal growth factor receptors. *Mol Biol Med* 1:511–529.
5. Lamborn KR, et al.North American Brain Tumor Consortium (2008) Progression-free survival: An important end point in evaluating therapy for recurrent high-grade gliomas. *Neuro-oncol* 10:162–170.
6. Huang PH, Xu AM, White FM (2009) Oncogenic EGFR signaling networks in glioma. *Sci Signal* 2:re6.
7. Kroll RA, Neuwelt EA (1998) Outwitting the blood-brain barrier for therapeutic purposes: Osmotic opening and other means. *Neurosurgery* 42:1083–1099, discussion 1099–1100.
8. Holliger P, Hudson PJ (2005) Engineered antibody fragments and the rise of single domains. *Nat Biotechnol* 23:1126–1136.
9. Muyldermans S (2001) Single domain camel antibodies: Current status. *J Biotechnol* 74:277–302.
10. Dolk E, et al. (2005) Induced refolding of a temperature denatured llama heavy-chain antibody fragment by its antigen. *Proteins* 59:555–564.
11. Stijlemans B, et al. (2004) Efficient targeting of conserved cryptic epitopes of infectious agents by single domain antibodies. African trypanosomes as paradigm. *J Biol Chem* 279:1256–1261.
12. Roovers RC, et al. (2007) Efficient inhibition of EGFR signaling and of tumour growth by antagonistic anti-EFGR Nanobodies. *Cancer Immunol Immunother* 56:303–317.
13. Aboody KS, et al. (2000) Neural stem cells display extensive tropism for pathology in adult brain: Evidence from intracranial gliomas. *Proc Natl Acad Sci USA* 97:12846–12851.
14. Tang Y, et al. (2003) In vivo tracking of neural progenitor cell migration to glioblastomas. *Hum Gene Ther* 14:1247–1254.
15. Shah K (2011) Mesenchymal stem cells engineered for cancer therapy. *Adv Drug Deliv Rev* 64:739–748.
16. Sasportas LS, et al. (2009) Assessment of therapeutic efficacy and fate of engineered human mesenchymal stem cells for cancer therapy. *Proc Natl Acad Sci USA* 106:4822–4827.
17. Kauer TM, Figueiredo JL, Hingtgen S, Shah K (2012) Encapsulated therapeutic stem cells implanted in the tumor resection cavity induce cell death in gliomas. *Nat Neurosci* 15:197–204.
18. Carrasco-García E, et al. (2011) Small tyrosine kinase inhibitors interrupt EGFR signaling by interacting with erbB3 and erbB4 in glioblastoma cell lines. *Exp Cell Res* 317: 1476–1489.
19. Hasselbalch B, et al. (2010) Prospective evaluation of angiogenic, hypoxic and EGFR-related biomarkers in recurrent glioblastoma multiforme treated with cetuximab, bevacizumab and irinotecan. *APMIS* 118:585–594.
20. Hasselbalch B, et al. (2010) Cetuximab, bevacizumab, and irinotecan for patients with primary glioblastoma and progression after radiation therapy and temozolomide: A phase II trial. *Neuro-oncol* 12:508–516.
21. Abulrob A, Sprong H, Van Bergen en Henegouwen P, Stanimirovic D (2005) The blood-brain barrier transmigrating single domain antibody: Mechanisms of transport and antigenic epitopes in human brain endothelial cells. *J Neurochem* 95:1201–1214.
22. Gainkam LO, et al. (2008) Comparison of the biodistribution and tumor targeting of two 99mTc-labeled anti-EGFR nanobodies in mice, using pinhole SPECT/micro-CT. *J Nucl Med* 49:788–795.
23. Corsten MF, Shah K (2008) Therapeutic stem-cells for cancer treatment: Hopes and hurdles in tactical warfare. *Lancet Oncol* 9:376–384.
24. Pandita A, Aldape KD, Zadeh G, Guha A, James CD (2004) Contrasting in vivo and in vitro fates of glioblastoma cell subpopulations with amplified EGFR. *Genes Chromosomes Cancer* 39:29–36.
25. Vivanco I, et al. (2010) The phosphatase and tensin homolog regulates epidermal growth factor receptor (EGFR) inhibitor response by targeting EGFR for degradation. *Proc Natl Acad Sci USA* 107:6459–6464.
26. Kokubo Y, et al. (2005) Reduction of PTEN protein and loss of epidermal growth factor receptor gene mutation in lung cancer with natural resistance to gefitinib (IRESSA). *Br J Cancer* 92:1711–1719.
27. Sos ML, et al. (2009) PTEN loss contributes to erlotinib resistance in EGFR-mutant lung cancer by activation of Akt and EGFR. *Cancer Res* 69:3256–3261.
28. Loew S, Schmidt U, Unterberg A, Halatsch ME (2009) The epidermal growth factor receptor as a therapeutic target in glioblastoma multiforme and other malignant neoplasms. *Anticancer Agents Med Chem* 9:703–715.
29. Dancey G, Begent RH, Meyer T (2009) Imaging in targeted delivery of therapy to cancer. *Target Oncol* 4:201–217.
30. Oliveira S, et al. (2012) Rapid visualization of human tumor xenografts through optical imaging with a near-infrared fluorescent anti-epidermal growth factor receptor nanobody. *Mol Imaging* 11:33–46.
31. Hingtgen SD, Kasmieh R, van de Water J, Weissleder R, Shah K (2010) A novel molecule integrating therapeutic and diagnostic activities reveals multiple aspects of stem cell-based therapy. *Stem Cells* 28:832–841.
32. Kim KM, et al. (2008) Anti-CD30 diabody-drug conjugates with potent antitumor activity. *Mol Cancer Ther* 7:2486–2497.